T2R2 東京科学大学 リサーチリポジトリ
Science Tokyo Research Repository

論文 / 著書情報
Article / Book Information

Title	Intentionally inserted oxygen depleted (Ba0.5Sr0.5)TiO3 layers as a model of DC-electrical degradation
Author	Toru Hara
Journal/Book name	IEEE Trans. Device Mater. Reliab., vol. 4, , p. 670
発行日 / Issue date	2004, 12
権利情報 / Copyright	(c)2004 IEEE. Personal use of this material is permitted. However, permission to reprint/republish this material for advertising or promotional purposes or for creating new collective works for resale or redistribution to servers or lists, or to reuse any copyrighted component of this work in other works must be obtained from the IEEE.

Powered by T2R2 (Science Tokyo Research Repository)

Intentionally Inserted Oxygen Depleted $(Ba_{0.5}Sr_{0.5})TiO_3$ Layers as a Model of DC-Electrical Degradation

Toru Hara, *Member, IEEE*

***Abstract*—The relative dielectric constant versus voltage ($\varepsilon_r - V$) characteristics and the current density versus electric field ($J - E$) characteristics of $(Ba_{0.5}Sr_{0.5})TiO_3$ films, which have intentionally inserted oxygen depleted layers near the bottom electrodes, were investigated as a model of dc-electrical degradation phenomena. Our investigation demonstrated that the intentionally inserted oxygen depleted layer is the cause of the tunneling conduction.**

***Index Terms*—Dielectric devices, dielectric polarization.**

I. Introduction

THE $(Ba, Sr)TiO_3$ (BST) thin films have attracted great attention for practical use in capacitors of dynamic random-access memories (DRAMs) in future gigabit DRAM generations. To use BST films for DRAMs, leakage currents must be kept sufficiently low such that capacitors do not discharge before they are refreshed. It is well known that the insulation resistance of BST thin film deteriorates due to oxygen vacancies.

A lot of work has been reported on leakage behaviors of BST thin films. Tsai and Tseng reported that the leakage currents of BST thin films abide by the interface-limited Schottky emission in a low-electric-field region, and by the bulk-limited Poole–Frenkel conduction in a high-electric-field region [1]. Furthermore, Shye *et al.* reported that the applied electric field boundary between the Schottky emission region and the Poole–Frenkel region shifted to a higher electric field as the $O_2/(Ar + O_2)$ mixing ratio (OMR) during sputtering increased, due to the compensation of oxygen vacancies [2]. It is assumed that the OMR of 20% is the threshold for the fabrication of high-quality BST films [2]. Shin *et al.* suggested the combined injection currents over the Schottky barrier (Schottky emission) and through the Schottky barrier (tunneling) [3]. According to this combined mechanism, it is predicted that the contribution of tunneling will increase if oxygen vacancies in BST films increase. We investigated the leakage behaviors of the dc-electrically degraded BST film and the BST film with intentionally inserted oxygen depleted layer, and confirmed that the dc-electrically degraded BST film exhibited analogous leakage behaviors with the BST film with intentionally inserted oxygen depleted layer [4].

Manuscript received April 10, 2004; revised July 13, 2004.

The author is with Taiyo Yuden Company, Ltd., Gunma-Gun, Gunma 370-3347, Japan (e-mail: thara@m6.dion.ne.jp).

Digital Object Identifier 10.1109/TDMR.2004.838421

A lot of work has been reported on the capacitance versus voltage characteristics of BST thin films. Maruno *et al.* fabricated Pt/BST with intentionally introduced oxygen vacancies at the surface of BST film by annealing under high vacuum condition/Pt capacitor, and confirmed the peak shift of a voltage, at which a capacitance has its maximum value, toward the negative-bias region [5]. Zafer *et al.* confirmed the peak shift of a voltage, at which a capacitance has its maximum value, toward the positive-bias region for the degraded specimen after applying constant voltage stress at a top electrode [6].

In order to fabricate high-quality BST films, it is important to understand the influence of oxygen vacancies near the interface between BST films and electrodes. Therefore, we fabricated Pt/BST with intentionally inserted oxygen depleted layer/Pt capacitors, and investigated their electrical characteristics. The present discussion concentrates on the effect of the intentionally introduced oxygen vacancies near the interface between BST films and electrodes.

II. Capacitor Fabrication

$Pt/(Ba_{0.5}Sr_{0.5})TiO_3/Pt$ capacitors and $Pt/(Ba_{0.5}Sr_{0.5})TiO_3$/oxygen-depleted $(Ba_{0.5}Sr_{0.5})TiO_3/Pt$ capacitors were prepared for electrical characteristics measurements.

The 250-nm-thick Pt films were deposited as bottom electrodes on $TiO_2(2\ nm)/SiO_2(80\ nm)/Si$ substrates at 250 °C by dc sputtering.

The single-layered $(Ba_{0.5}Sr_{0.5})TiO_3$ films without intentionally introduced oxygen vacancies were deposited to the thicknesses of 40, 62, 89, 102, 117, 166, 185, 308, and 405 nm by RF magnetron sputtering. The $(Ba_{0.5}Sr_{0.5})TiO_3$ films without intentionally introduced oxygen vacancies were deposited on the Pt bottom electrodes. Oxygen mixing ratio (OMR) was maintained at 50% when the $(Ba_{0.5}Sr_{0.5})TiO_3$ layers were deposited. To investigate the influence of $(Ba_{0.5}Sr_{0.5})TiO_3$ thickness on the relative dielectric constant, the 40-, 62-, 89-, 102-, 117-, 166-, 308-, and 405-nm-thick $(Ba_{0.5}Sr_{0.5})TiO_3$ films without intentionally introduced oxygen vacancies were deposited. These results are shown in Fig. 4(a). Experimental details are described in [10]. The 185-nm-thick $(Ba_{0.5}Sr_{0.5})TiO_3$ film without intentionally introduced oxygen vacancies is a control for the comparison with the $(Ba_{0.5}Sr_{0.5})TiO_3$ films, which have intentionally inserted oxygen depleted layers, with the total thicknesses of 185 nm.

The double-layered $(Ba_{0.5}Sr_{0.5})TiO_3$ films were deposited to a total thickness of 185 nm by RF magnetron sputtering.

1530-4388/$20.00 © 2004 IEEE

Authorized licensed use limited to: TOKYO INSTITUTE OF TECHNOLOGY. Downloaded on July 24, 2009 at 01:58 from IEEE Xplore. Restrictions apply.

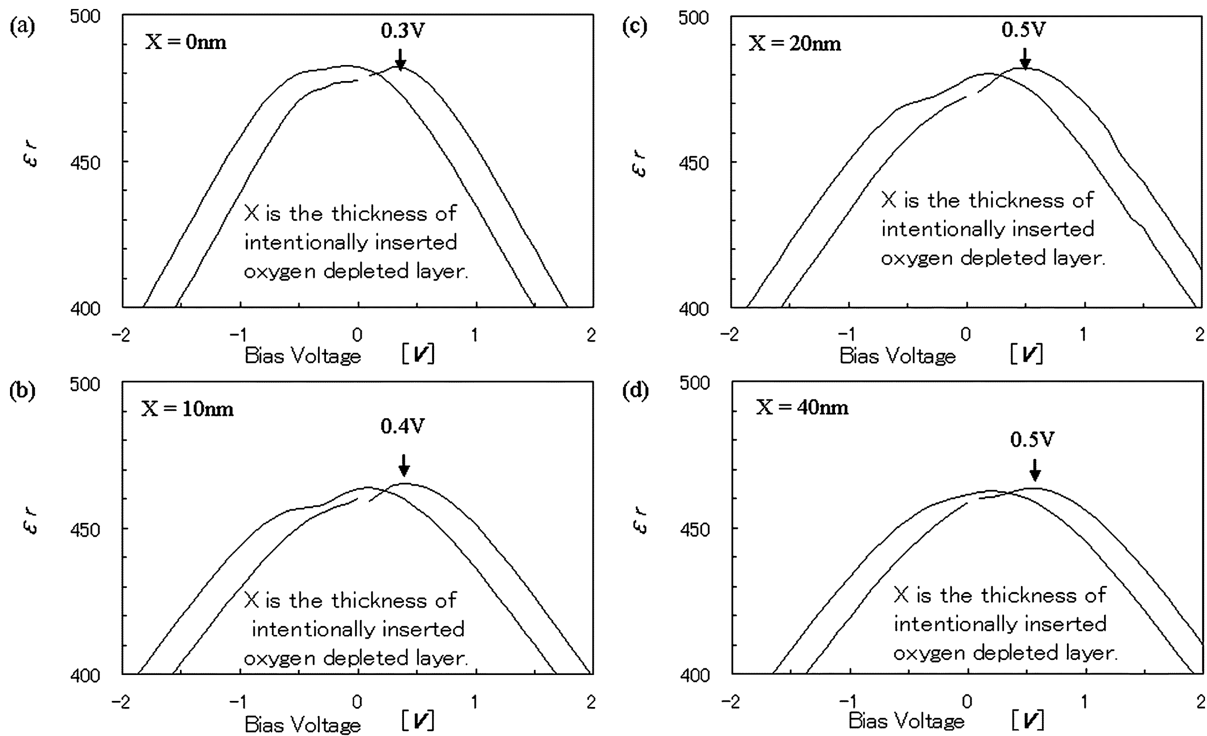

Fig. 1. Plots of relative dielectric constant (ε_r) versus voltage (V) for test capacitors. Each plot shows ε_r versus V for the specimen without intentionally inserted oxygen depleted $(Ba_{0.5}Sr_{0.5})TiO_3$ layer and the specimen with intentionally inserted oxygen depleted $(Ba_{0.5}Sr_{0.5})TiO_3$ layer with a thickness of (a) $X = 0$ nm, (b) $X = 10$ nm, (c) $X = 20$ nm, and (d) $X = 40$ nm. X is the thickness of intentionally inserted oxygen depleted $(Ba_{0.5}Sr_{0.5})TiO_3$ layer. The $(Ba_{0.5}Sr_{0.5})TiO_3$ films were deposited to a total thickness of 185 nm.

TABLE I
PHYSICAL ATTRIBUTES OF THE TEST CAPACITORS HAVING THE DOUBLE-LAYERED $(Ba_{0.5}Sr_{0.5})TiO_3$ FILMS

Top Electrode :	Pt
2nd Dielectric Film :	$(Ba_{0.5}Sr_{0.5})TiO_3$
	Thickness: (1) 175*nm*, (2) 165*nm*, (3) 145*nm*
1st Dielectric Film :	$(Ba_{0.5}Sr_{0.5})TiO_3$ with intentionally introduced oxygen vacancies
	Thickness: (1) 10*nm*, (2) 20*nm*, (3) 40*nm*
Bottom Electrode :	Pt

First, the 10-, 20-, or 40-nm-thick $(Ba_{0.5}Sr_{0.5})TiO_3$ films with intentionally introduced oxygen vacancies [oxygen depleted $(Ba_{0.5}Sr_{0.5})TiO_3$] were deposited on Pt bottom electrodes. OMR was maintained at 0% when the first $(Ba_{0.5}Sr_{0.5})TiO_3$ layers were deposited. Second, the 175-, 165-, or 145-nm-thick $(Ba_{0.5}Sr_{0.5})TiO_3$ films without intentionally introduced oxygen vacancies were deposited on the oxygen depleted $(Ba_{0.5}Sr_{0.5})TiO_3$. OMR was maintained at 50% when the second $(Ba_{0.5}Sr_{0.5})TiO_3$ layers were deposited. Table I shows the physical attributes of the test capacitors having the double-layered $(Ba_{0.5}Sr_{0.5})TiO_3$ films.

All $(Ba_{0.5}Sr_{0.5})TiO_3$ films were prepared at a fixed RF power of 1 kW and a fixed dc power of 200 W. A constant pressure of 0.035 Pa and a constant substrate temperature of 600 °C were maintained during the deposition of $(Ba_{0.5}Sr_{0.5})TiO_3$ films.

The 250-nm-thick Pt films were deposited as top electrodes with a diameter of 0.5 mm on the $(Ba_{0.5}Sr_{0.5})TiO_3$ films by electron beam evaporation at 120 °C, using a metal shadow mask.

After a series of depositions, the capacitors were annealed at 600 °C in oxygen ambient for 30 min to introduce oxygen into the surface of the $(Ba_{0.5}Sr_{0.5})TiO_3$ films [7]. In the negatively biased region [electrons are injected from the top electrodes to the second $(Ba_{0.5}Sr_{0.5})TiO_3$ layers], leakage currents of the specimens are decreased by post-annealing.

Thickness measurements were performed using a spectroscopic ellipsometer.

III. ELECTRICAL CHARACTERIZATION

The relative dielectric constant versus voltage $(\varepsilon_r - V)$ curves at 10 kHz were obtained using an HP4284A precision LCR meter. The measuring frequency of 10 kHz was selected to reduce the influence of low-frequency dielectric dispersion [9]. The sweep rate was set at 0.2 V/s, with an ac-bias of 100 mV. The measuring ac-bias of 100 mV was selected to reduce the influence of ac-bias on dc-bias. The dc-bias voltage was swept from the zero-bias region to the positive-bias region, returned to the zero-bias region, swept from the zero-bias region to the negative-bias region, and finally returned to the zero-bias region. The $\varepsilon_r - V$ measurements were performed at 40 °C.

The current density versus electric field $(J - E)$ characteristics was measured using a pA-meter (ADVANTEST R62469) through a step voltage technique with stair-shaped dc-bias voltage applied to the top electrode, while the bottom electrode was grounded. The value of each voltage step and the hold

Authorized licensed use limited to: TOKYO INSTITUTE OF TECHNOLOGY. Downloaded on July 24, 2009 at 01:58 from IEEE Xplore. Restrictions apply.

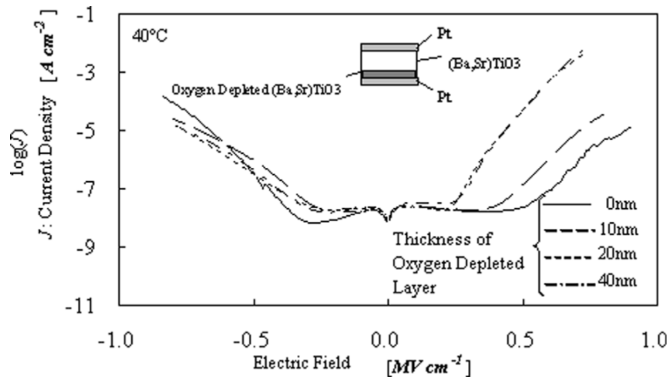

Fig. 2. Plots of current density (J) at 40 °C versus electric field (E) for a $Pt/(Ba_{0.5}Sr_{0.5})TiO_3/Pt$ capacitor and for $Pt/(Ba_{0.5}Sr_{0.5})TiO_3/$ oxygen depleted $(Ba_{0.5}Sr_{0.5})TiO_3/Pt$ capacitors. The $(Ba_{0.5}Sr_{0.5})TiO_3$ films were deposited to a total thickness of 185 nm.

time were 0.1 V and 1 s, respectively. In order to minimize the influence of the relaxation current on the leakage current data, measurement was performed after sweeping the voltage to the maximum value of each biased direction. The $J-E$ measurements were performed at 40 °C, at 60 °C, and at 80 °C.

IV. Relative Dielectric Constant—Applied Voltage Characteristics

Fig. 1 shows the plots of relative dielectric constant (ε_r) versus applied voltage (V).

As shown in Fig. 1(a), the voltage peak was shifted toward the positive-bias region in the sample without intentionally introduced oxygen vacancies. It is assumed that the voltage shift in the sample without intentionally introduced oxygen vacancies is due to the native positively charged defects such as oxygen vacancies, and due to the ferroelectricity induced by the incorporation of Ba into the $SrTiO_3$ lattice.

As shown in Fig. 1(b), (c), and (d), the voltages at which the relative dielectric constants have their maximum values of $Pt/(Ba_{0.5}Sr_{0.5})TiO_3$/oxygen depleted $(Ba_{0.5}Sr_{0.5})TiO_3/Pt$ specimens were shifted toward the positive-bias region compared with that of $Pt/(Ba_{0.5}Sr_{0.5})TiO_3/Pt$ specimen. This can be attributed to positively charged oxygen vacancies near the bottom electrodes. These results were in good agreement with the results of previous work [5], [6]. The peak shift of a voltage toward the positive-bias region (ΔV_m), at which a capacitance has its maximum value, increases in accordance with the increasing thickness of intentionally inserted oxygen depleted $(Ba_{0.5}Sr_{0.5})TiO_3$ layer. However, when the thickness of the intentionally inserted oxygen depleted $(Ba_{0.5}Sr_{0.5})TiO_3$ layer exceeds 20 nm, ΔV_m tends to be saturated, as shown in Fig. 1(c) and (d).

V. Current Density—Applied Electric Field Characteristics

Fig. 2 shows the plots of current density (J) at 40 °C versus mean applied electric field (E) across the $(Ba_{0.5}Sr_{0.5})TiO_3$ film.

As shown in Fig. 2, in the positively biased region [electrons are injected from the bottom electrodes to

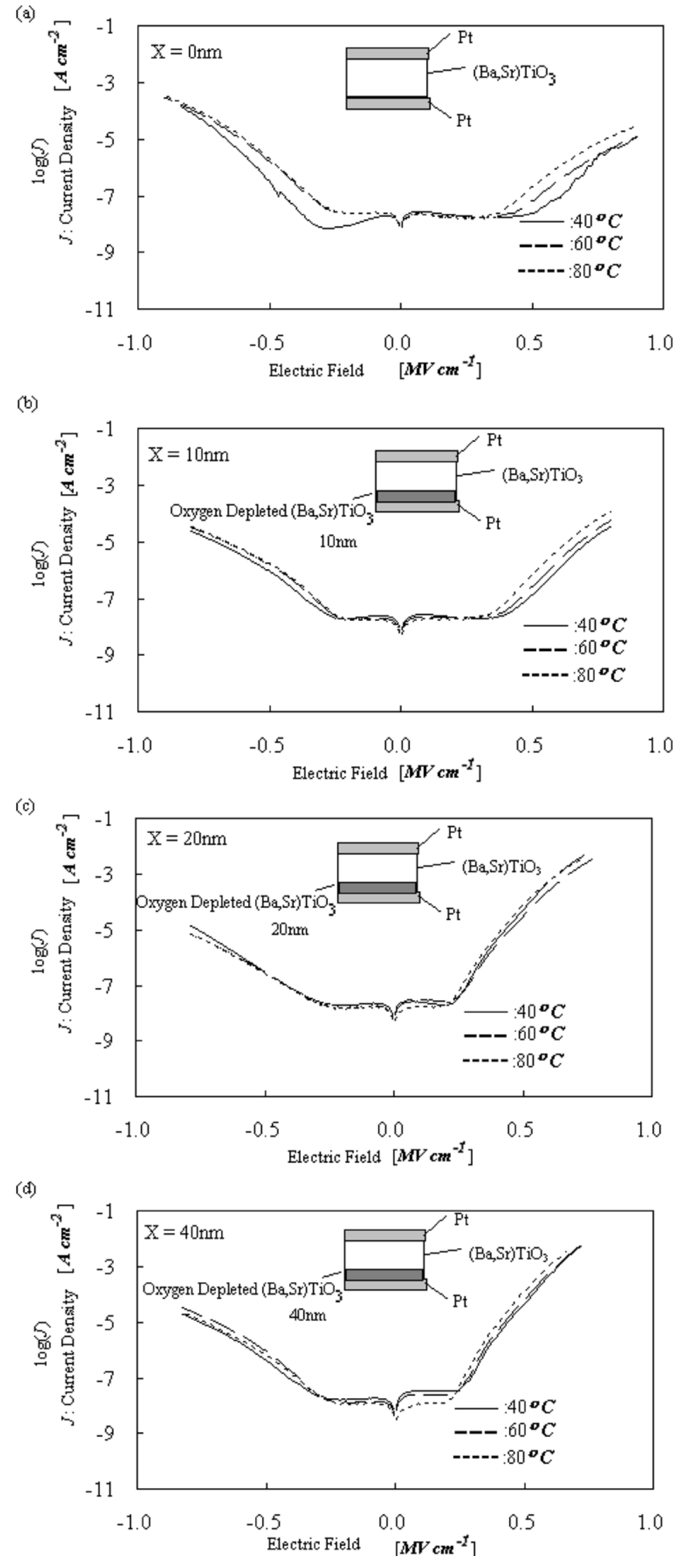

Fig. 3. Plots of current density (J) at 40–80 °C versus electric field (E) for test capacitors. Each plot shows J versus E for the specimen without intentionally inserted oxygen depleted $(Ba_{0.5}Sr_{0.5})TiO_3$ layer and the specimen with intentionally inserted oxygen depleted $(Ba_{0.5}Sr_{0.5})TiO_3$ layer with a thickness of (a) $X = 0$ nm, (b) $X = 10$ nm, (c) $X = 20$ nm, and (d) $X = 40$ nm. X is the thickness of intentionally inserted oxygen depleted $(Ba_{0.5}Sr_{0.5})TiO_3$ layer.

the $(Ba_{0.5}Sr_{0.5})TiO_3$ films], the leakage currents of $Pt/(Ba_{0.5}Sr_{0.5})TiO_3$/oxygen depleted $(Ba_{0.5}Sr_{0.5})TiO_3/Pt$

Authorized licensed use limited to: TOKYO INSTITUTE OF TECHNOLOGY. Downloaded on July 24, 2009 at 01:58 from IEEE Xplore. Restrictions apply.

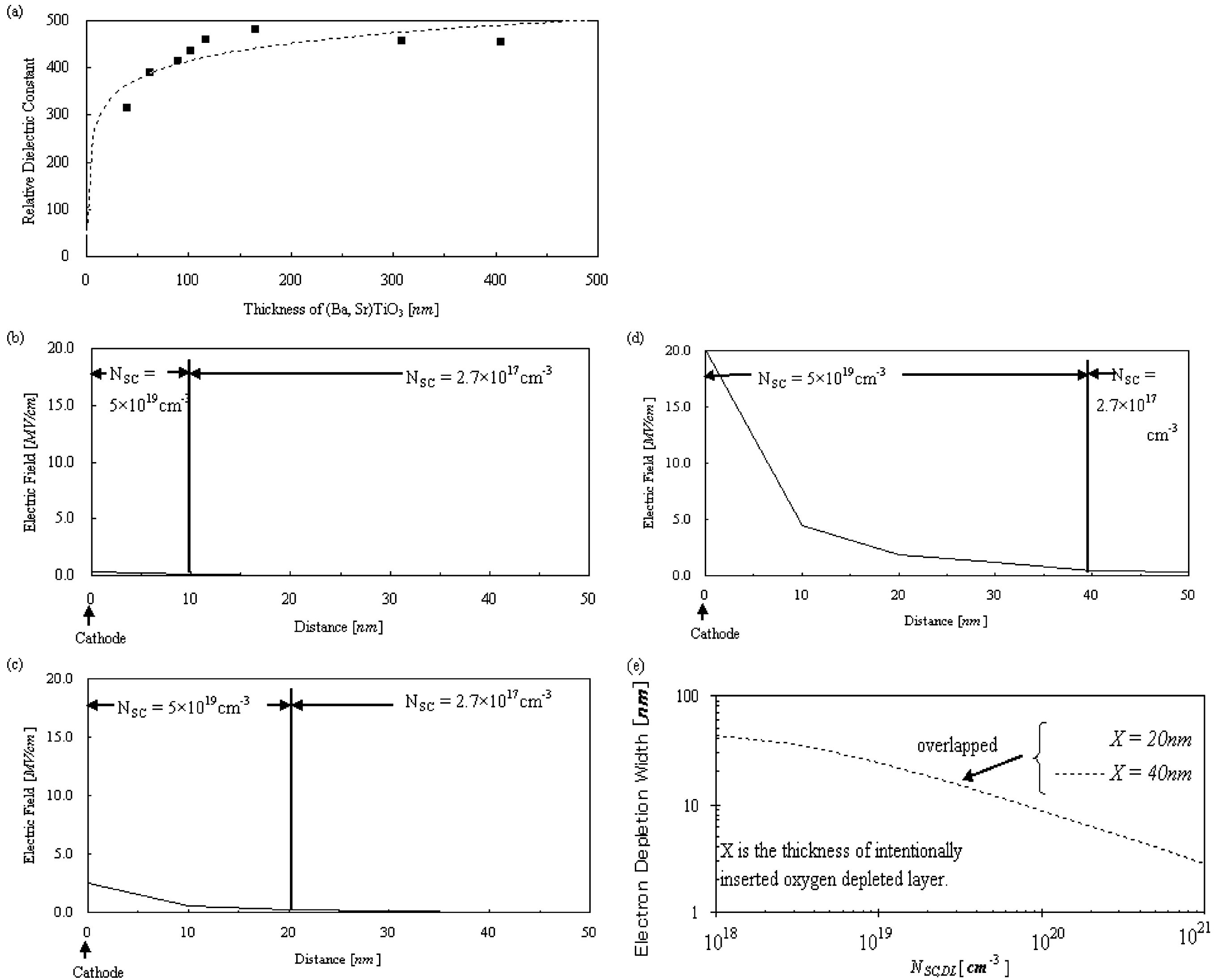

Fig. 4. (a) Plots of measured relative dielectric constant versus the thickness of $(Ba_{0.5}Sr_{0.5})TiO_3$ film without intentionally inserted oxygen depleted layer. The maximum values of relative dielectric constants were shown. Details were described in [10]. (b)–(c) Plots of electric field near the interface between the oxygen depleted $(Ba_{0.5}Sr_{0.5})TiO_3$ layer and the cathode as a function of positive space-charge density (N_{SC}). The thickness of intentionally inserted oxygen depleted $(Ba_{0.5}Sr_{0.5})TiO_3$ layer (X) is (b) 10 nm, (c) 20 nm, and (d) 40 nm. The maximum values of relative dielectric constants were used for the calculation of electric field. (e) Plots of estimated electron depletion width (W) as a function of the positive space-charge density in the electron depletion layer $(N_{SC,DL})$. A parameter of $N_{SC,DL}$, which has been varied from 1×10^{24} m^{-3} to 1×10^{27} m^{-3} in order to simulate the effects of oxygen vacancies, is external.

specimens increase more than that of $Pt/(Ba_{0.5}Sr_{0.5})TiO_3/Pt$ specimen. However when the thickness of oxygen depleted $(Ba_{0.5}Sr_{0.5})TiO_3$ layer exceeds 20 nm, the leakage current was independent of the thickness of oxygen depleted $(Ba_{0.5}Sr_{0.5})TiO_3$ layer.

As shown in Fig. 2, in the negatively biased region [electrons are injected from the top electrodes to the $(Ba_{0.5}Sr_{0.5})TiO_3$ films], the leakage currents of $Pt/(Ba_{0.5}Sr_{0.5})TiO_3)TiO_3$/oxygen depleted $(Ba_{0.5}Sr_{0.5})TiO_3/Pt$ specimens are comparable with that of $Pt/(Ba_{0.5}Sr_{0.5})TiO_3/Pt$ specimen.

Fig. 3 shows the plots of current density (J) at 40–80 °C versus mean applied electric field (E) across the $(Ba_{0.5}Sr_{0.5})TiO_3$ film. Each plot shows J versus E for the specimen without oxygen depleted $(Ba_{0.5}Sr_{0.5})TiO_3$ layer [(a) $X = 0$ nm] and the specimen with oxygen depleted $(Ba_{0.5}Sr_{0.5})TiO_3$ layer with a thickness of (b) $X = 10$ nm, (c) $X = 20$ nm, and (d) $X = 40$ nm. X is the thickness of intentionally inserted oxygen depleted $(Ba_{0.5}Sr_{0.5})TiO_3$ layer.

In Fig. 3(a), there appears an asymmetry in the temperature dependent $J-E$ curves for the $(Ba_{0.5}Sr_{0.5})TiO_3$ film without intentionally introduced oxygen vacancies. This is probably due to the different thermal stresses of the top-Pt/bottom-Pt on the deposition of the $(Ba_{0.5}Sr_{0.5})TiO_3$ film, and due to the difference of oxygen incorporation during the post annealing.

As shown in Fig. 3(a), in the positively biased region [electrons are injected from the bottom electrodes to the $(Ba_{0.5}Sr_{0.5})TiO_3$ films], the leakage current of Pt/185-nm-thick $(Ba_{0.5}Sr_{0.5})TiO_3/Pt$ depends on temperature during the measurements. The leakage current in the positively biased region of Pt/175-nm-thick $(Ba_{0.5}Sr_{0.5})TiO_3$/10-nm-thick oxygen depleted $(Ba_{0.5}Sr_{0.5})TiO_3/Pt$ was less dependent of temperature during measurements, as shown in Fig. 3(b). Furthermore, as the thickness of the intentionally inserted oxygen depleted

Authorized licensed use limited to: TOKYO INSTITUTE OF TECHNOLOGY. Downloaded on July 24, 2009 at 01:58 from IEEE Xplore. Restrictions apply.

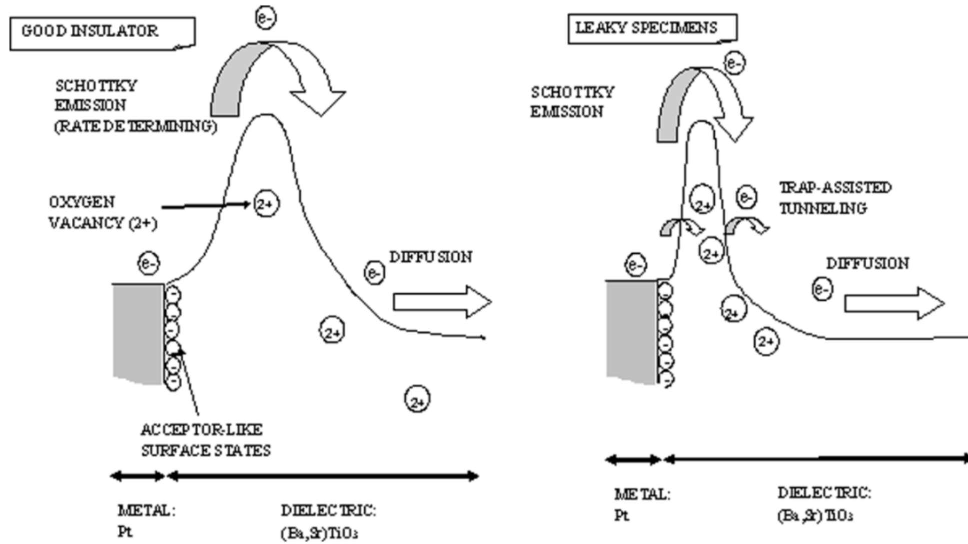

Fig. 5. Schematic energy-band diagrams to explain the thermionic emission mechanism and the tunneling mechanism. As mentioned tunneling contributions, it should be more important for leaky films.

$(Ba_{0.5}Sr_{0.5})TiO_3$ layer exceeds 20 nm, leakage currents in the positively biased region were independent of temperature during measurements, as shown in Fig. 3(c) and (d). This can be explained by assuming that the thermionically emitted electrons and tunneling electrons exist [3], and that the contribution of tunneling increases for the leaky specimens with intentionally inserted oxygen depleted layer.

VI. Discussion

Fig. 4(a) shows the plots of extracted maximum relative dielectric constant versus the thickness of $(Ba_{0.5}Sr_{0.5})TiO_3$ film without the intentionally inserted oxygen depleted layer.

Fig. 4(b), (c), and (d) shows the plots of electric field near the interface between the oxygen depleted $(Ba_{0.5}Sr_{0.5})TiO_3$ layer and the electrode (cathode) as a function of positive space-charge density.

The electric fields near the interface between oxygen depleted $(Ba_{0.5}Sr_{0.5})TiO_3$ layers and cathodes are given by

$$E = \frac{qN_{SC}t_{ODL}}{2\varepsilon_0\varepsilon_{ODL}}\left(1 + \frac{N_{SC,ODL}t_{ODL}^2}{N_{SC}t^2}\right) \quad (1)$$

where q is the magnitude of space-charge (space charge is the oxygen vacancy. $q = 2$), N_{SC} is the positive space charge density in the remaining film without the intentionally inserted oxygen depleted $(Ba_{0.5}Sr_{0.5})TiO_3$ layer, t_{ODL} is the thickness of intentionally inserted oxygen depleted $(Ba_{0.5}Sr_{0.5})TiO_3$ layer, ε_0 is the dielectric constant of free space, ε_{ODL} is the relative dielectric constant of intentionally inserted oxygen depleted $(Ba_{0.5}Sr_{0.5})TiO_3$ layer [estimated from Fig. 4(a)], $N_{SC,ODL}$ is the positive space-charge density in the intentionally inserted oxygen depleted $(Ba_{0.5}Sr_{0.5})TiO_3$ layer, and t is the distance from the cathode, respectively [5]. When we assume $N_{SC,ODL} = 5.0 \times 10^{19}$ cm^{-3} and $N_{SC} = 2.7 \times 10^{17}$ cm^{-3} [5], and assume $t_{ODL} = 10$ nm, the local electric field near the interface is very low, as shown in Fig. 4(b). However, when we assume $t_{ODL} = 20$–40 nm, the local electric fields near the interface increase, as shown in Fig. 4(c) and (d). It is assumed that the tunneling conduction shown in Fig. 3(c) and (d) is probably due to the electric field enhancement near the cathode shown in Fig. 4(c) and (d).

When the positively charged oxygen vacancies exist near the bottom electrode, the shift of the voltage (ΔV_m) toward the positive-bias region, at which the relative dielectric constant has its maximum value, is approximately expressed by

$$\Delta V_m = \frac{2e(N_{SC,DL})W^2}{2\varepsilon_0\varepsilon_{DL}} \quad (2)$$

where e is the elementary charge, ε_0 is the dielectric constant of free space, ε_{DL} is the relative dielectric constant of $(Ba_{0.5}Sr_{0.5})TiO_3$ films in the electron depletion layer $(\varepsilon_{DL} = \varepsilon_{ODL})$, $N_{SC,DL}$ is the positive space-charge density in the electron depletion layer $(N_{SC,DL} = N_{SC,ODL})$, and W is the electron depletion width, respectively [5]. The oxygen vacancies assumed to be immobile under our measurement conditions [10], [11], but the oxygen vacancies may migrate under a constant dc voltage stress at a high temperature [4], [6].

Fig. 4(e) shows the plots of estimated W extracted from (2) as a function of $N_{SC,DL}$. A parameter of $N_{SC,DL}$, which has been varied from 1.0×10^{18} cm^{-3} to 1.0×10^{21} cm^{-3} in order to simulate the effects of oxygen vacancies, is external. When $N_{SC,DL} = 5 \times 10^{19}$ cm^{-3}, $W = 12$ nm. This is in good agreement with the results in Fig. 4(c) and (d). These results show that our model is self-consistent.

It was considered that the negatively charged acceptor-like surface states pin the Fermi level of $(Ba,Sr)TiO_3$ thin film [2], [8]. Assuming the electronic structure near the cathode, positively charged oxygen vacancies near the cathode can compensate for the negative charges of acceptor-like surface states [2], [8]. Therefore, the electron depletion width of the leaky specimen may decrease due to high density of positively charged oxygen vacancies, as shown in Fig. 5. This may be the origin of tunneling conduction [2]. To investigate the electronic structure of oxygen depleted $(Ba,Sr)TiO_3$ films, it is anticipated that the magnetic field characterization using the electron paramagnetic resonance spectroscopy is an effective

Authorized licensed use limited to: TOKYO INSTITUTE OF TECHNOLOGY. Downloaded on July 24, 2009 at 01:58 from IEEE Xplore. Restrictions apply.

method. We hope to investigate the electronic structure of oxygen depleted $(Ba_{0.5}Sr_{0.5})TiO_3$ films in the future.

VII. CONCLUSION

Our investigation demonstrated that the oxygen depleted layer near the interface between the $(Ba_{0.5}Sr_{0.5})TiO_3$ film and the electrode is the cause of tunneling conduction. It is concluded that the sufficient OMR during the deposition of $(Ba_{0.5}Sr_{0.5})TiO_3$ films can be a process recipe guideline for the device manufacturing so as to avoid the degradation of capacitors with $(Ba_{0.5}Sr_{0.5})TiO_3$ films, as described in [1] and [2]. We hope that the above discussion will be useful for understanding the physical nature of the leakage behaviors and the dc-electrical degradation in capacitors with $(Ba_{0.5}Sr_{0.5})TiO_3$ films.

REFERENCES

[1] M. S. Tsai and T. Y. Tseng, "Conduction mechanism and temperature-dependent current-voltage in $(Ba, Sr)TiO_3$ thin films," *J. Electrochem. Soc.*, vol. 145, pp. 2853–2860, Aug. 1998.

[2] D.-C. Shye, B.-S. Chiou, M.-J. Lai, C.-C. Hwang, C.-C. Jiang, J.-S. Chen, M.-H. Cheng, and H.-C. Cheng, "Low temperature radio-frequency-sputtered $(Ba, Sr)TiO_3$ films on Pt/TiN/Ti/Si substrates with various oxygen/argon mixing ratios," *J. Electrochem. Soc.*, vol. 150, pp. F20–F27, 2003.

[3] J. C. Shin, J. Park, C. S. Hwang, and H. J. Kim, "Dielectric and electrical properties of sputter grown $(Ba, Sr)TiO_3$ thin films," *J. Appl. Phys.*, vol. 86, pp. 506–513, Jul. 1999.

[4] T. Hara, "Leakage behavior of dc-electrically-degraded $(Ba, Sr)TiO_3$ thin films," *IEEE Trans. Device Mater. Rel.*, vol. 4, no. 2, pp. 268–272, Jun. 2004.

[5] S. Maruno, T. Kuroiwa, N. Mikami, K. Sato, S. Ohmura, M. Kaida, T. Yasue, and T. Koshikawa, "Model of leakage characteristics of $(Ba, Sr)TiO_3$ thin films," *Appl. Phys. Lett.*, vol. 73, pp. 954–956, Aug. 1998.

[6] S. Zafer, B. Hradsky, D. Gentile, P. Chu, R. E. Jones, and S. Gillespie, "Resistance degradation in barium strontium titanate thin films," *J. Appl. Phys.*, vol. 86, pp. 3890–3894, Oct. 1999.

[7] J.-H. Joo, J.-M. Seon, Y.-C. Jeon, K.-Y. Oh, J.-S. Roh, and J.-J. Kim, "Improvement of leakage currents of $Pt/(Ba, Sr)TiO_3/Pt$ capacitors," *Appl. Phys. Lett.*, vol. 70, pp. 3053–3055, Jun. 1997.

[8] S. Hara, "The Schottky limit and a charge neutrality level found on metal/6H-SiC interfaces," *Surf. Sci. Lett.*, vol. 494, pp. L805–L810, 2001.

[9] N. Cramer, T. S. Kalkur, E. Philofsky, and L. Kammerdiner, "An equivalent circuit model for $Ba_{.5}Sr_{.5}TiO_3$-based capacitors," *Integrat. Ferroelectr.*, vol. 58, pp. 1395–1402, 2003.

[10] T. Hara, "Electrical characteristics of $(Ba, Sr)TiO_3$ films accounted by partially depleted model," *Microelectron. Eng.*, vol. 75, pp. 316–320, 2004, to be published.

[11] T. Hara, "Electron-detrapping from localized states in the band gap of $(Ba, Sr)TiO_3$," *Solid State Commun.*, vol. 132, pp. 109–114, 2004, to be published.

Toru Hara (M'03) was born in Shimane-Ken, Japan, in 1968. He received the M.S. degree in chemistry from Hiroshima University, Japan, in 1993.

His major research interest is in the area of thin dielectric films. In particular, he is engaged in the characterization and modeling of the oxide failure (degradation and breakdown).

Mr. Hara is a member of the Electrochemical Society and the Japan Society of Applied Physics.

Authorized licensed use limited to: TOKYO INSTITUTE OF TECHNOLOGY. Downloaded on July 24, 2009 at 01:58 from IEEE Xplore. Restrictions apply.